

Proceeding Paper

Gold Nanostructure Orchestrated Electrochemical Immunosensor Integrated with Antibody-Electroactive Probe Conjugate for Rapid Detection of SARS-CoV2 Antibody[†]

Asmita Gupta, Chansi and Tinku Basu*

¹Amity Centre for Nanomedicine, Amity University, Noida 201301, Uttar Pradesh, India; agupta17@amity.edu (A.G.); cgupta2@amity.edu (C.)

* Correspondence: tbasu@amity.edu.

[†] Presented at the 3rd International Electronic Conference on Biosensors, 8–21 May 2023; Available online: <https://iecb2023.sciforum.net>.

Abstract: Viral detection has been studied predominantly in the last few years with the morbid spread of COVID-19. Biosensors have been widely used for the detection of various biological molecules, show a high potential for miniaturization and a friendly approach towards detection. Nano-materials play a significant role in the development of biosensing devices owing to their distinct morphological, optical, electrical, chemical, and physical properties, improving the sensing efficiency. Therefore, the present work reports the fabrication of an electrochemical immunosensor adorned with gold nanoparticles coupled to a redox indicator labeled antibody conjugate for rapid detection of SARS-CoV2 antibodies. The fabricated immunosensor can detect SARS-CoV2 antibodies within a linear detection range of 10–100 ngmL⁻¹ and offer a sensitivity of 0.013 × 10⁻³ mA ng⁻¹mLmm⁻². The adopted concept can be extended further for the detection of other viral antibodies with high sensitivity, and display high prospects for miniaturization, hence offering a huge commercialization potential.

Citation: Gupta, A.; Chansi; Basu, T. Gold Nanostructure Orchestrated Electrochemical

Immunosensor Integrated with Antibody-Electroactive Probe Conjugate for Rapid Detection of SARS-CoV2 Antibody. *Eng. Proc.* **2023**, *35*, x. <https://doi.org/10.3390/xxxxx>

Published: 22 May 2023

Publisher's Note: MDPI stays neutral concerning jurisdictional claims in published maps and institutional affiliations.



Copyright: Copyright: © 2023 by the authors. Submitted for possible open access publication under the terms and conditions of the Creative Commons Attribution (CC BY) license (<https://creativecommons.org/licenses/by/4.0/>).

Keywords: SARS-CoV2 ; electrochemical biosensor; gold nanoparticles; conjugate

1. Introduction

Severe acute respiratory syndrome 2 (SARS-CoV2) being a causative agent of coronavirus disease (COVID-19) poses a grave impact on individual health. It is a single-stranded RNA virus belonging to the Sarbecovirus subgenus of the Betacoronavirus genus. The basic structural proteins of the virus are spike protein(S), an envelope protein(E), and nucleocapsid protein(N). [1] The receptor binding domain of the Spike protein attacks the Angiotensin-Converting enzyme 2(ACE-2) present in the lung, entering endocytosis causing fever, cold, cough in mild cases, to severe lung infection, myocardial infection, kidney, heart, or multiple organ failure in severe cases [2,3].

Though, RT-PCR remains the gold standard for the confirmation of the disease; specific lab requirements, such as sub-zero temperature, long reaction time, need for a trained technician, etc. hurdles the scrutiny of the disease amongst the masses. Thus, for the initial screening of patients, point of care (PoC) devices such as lateral flow immunoassays based on reversed affinity between receptor-ligand interaction have been developed for rapid, on-site, self-monitoring by the people [4–6]. However, these devices are qualitative and have a high limit of detection due to which they are prone to show false-negative and positive results in cases with a lower concentration of antibodies in the sample and display cross reactivity.

Recently, biosensors with optical, colorimetric, piezoelectric, and electrochemical readouts have been reported for the detection of antibodies in the blood, serum, saliva, nasopharyngeal and oropharyngeal samples. Electrochemical biosensors have a well-established reputation for high accuracy, sensitivity, and precise diagnosis [7–9]. Furthermore, on modification with nanomaterials, they tend to show an overall enhancement in the diagnosis [10–13]. Gold nanomaterials (nanoparticles, nano-flowers, magnetic nanobeads, nanocomposites, etc.) have been widely reported to improve the efficiency of various sensing technologies. Apart from improving the interface properties they can also be easily functionalized and conjugated to biomolecules to serve as a reporter. [14–18]

Thus, to monitor and meet the global exigency for rapid, reliable, and early-stage diagnosis of COVID-19 in the present study we have fabricated an electrochemical immunosensor decorated with gold nanoparticles and electroactive probe conjugate for quantitative estimation of SARS-CoV2 antibodies. The sensor offers a linear detection range of 10 to 100 ng mL⁻¹, low limit of detection (LOD=3.59 ng mL⁻¹), high linearity R²=0.96, and sensitivity of 0.013 × 10⁻³ mA ng⁻¹ mL mm⁻². The immunosensor shows excellent stability for a month. The quantitative estimation for SARS-CoV2 antibody can be useful for sero-surveillance studies in the future.

2. Materials

For the immunosensor fabrication and characterization; nafion (5%, SRL), SARS-CoV2 spike protein (Sigma Aldrich), monoclonal antibody against SARS-CoV2 (Sigma Aldrich), BSA (Bovine Serum Albumin, SRL); horseradish peroxidase tagged secondary antibody (HRP-pAb) (Sigma Aldrich) Hydrogen peroxide (H₂O₂) (30%, Fisher Scientific), Chloroauric acid (HAuCl₄, Sigma Aldrich), Trisodium citrate dihydrate (SRL), Potassium Ferrocyanide (Fisher Scientific), Potassium Ferricyanide (Fisher Scientific) were purchased.

3. Methodology

Gold nanoparticles were first prepared using the Turkevich method [19–21]. The immunosensor was fabricated onto the conducting ITO-coated glass as a base electrode. The electrodes were washed by ultrasonication using acetone, ethanol, and water (10 min each). A polymeric solution of 1% nafion was spin-coated onto the conducting surface of the ITO to form a uniform layer (nf/ITO) eventually modified with a layer of synthesized gold nanoparticles (AuNPs) to obtain AuNPs/nf/ITO surface. Following this the capture probe was immobilized onto the surface of AuNPs/nf/ITO. The concentration and incubation time of the capture probe (Spro) was optimized prior to immobilization. Non-specific binding sites of the capture probe were then blocked by incubating Spro/AuNPs/nf/ITO with BSA (1 mg/ml) for 45 min. The fabricated immunosensor probe BSA/Spro/AuNPs/nf/ITO was then used to detect specific antibodies (CoV2-Ab) against SARS-CoV2, in the sample. A signal probe i.e HRP tagged secondary antibody (HRP-pAb), was incubated with CoV2-Ab/BSA/Spro/AuNPs/nf/ITO to form the immunosensor (HRP-pAb/CoV2-Ab/BSA/Spro/AuNPs/nf/ITO). After each modification, the electrodes were washed with PBS (Phosphate Buffer Saline), to remove the unbound molecules, finally the electrodes were stored at 4 °C till further use. The electrodes were electrochemically characterized for each layer. The response study of BSA/Spro/AuNPs/nf/ITO was noted for different concentrations of CoV2-Ab. H₂O₂ was used as a substrate to activate HRP-pAb/CoV2-Ab/BSA/Spro/AuNPs/nf/ITO immunosensor. Therefore, before the response study, the concentration and volume of H₂O₂ (5%, 200 μl) were optimized. The electrochemical response of HRP-pAb/CoV2-Ab/BSA/Spro/AuNPs/nf/ITO was recorded for different concentrations of CoV2-Ab and the calibration curve was formed. To study the stability of the immunosensor; thirty immunosensor (HRP-pAb/CoV2-Ab/BSA/Spro/AuNPs/nf/ITO) were prepared and stored at 4 °C and their electrochemical response was recorded at regular intervals for 30 days.

4. Characterization

UV-Visible spectroscopy was performed using Hitachi U3300 Spectrophotometer for the optical characterization of gold nanoparticles. A stand-alone Potentiostat/Galvano stat; Auto lab workstation MAC90135 procured from Metrohm, guided by NOVA 2.1 software was used to perform Differential Pulse Voltammetry for electrochemical characterization, response study of the fabricated HRP-pAb/CoV2-Ab/BSA/Spro/AuNPs/nf/ITO immunosensor. To perform the electrochemistry a three-electrode electrochemical cell was utilized; wherein the fabricated immunosensor probe was used as the working electrode, Platinum electrode (Pt) as the counter, and Ag/AgCl as the reference electrodes. The testing was done in PBS solution with 5mM Ferro/Ferricyanide solution $[\text{Fe}(\text{CN})_6]^{3-/4-}$ and the changes in the current response were noted for the analysis.

5. Result and Discussion

5.1. Gold Nanoparticles Characterization

5.1.1. UV-Visible Spectroscopy

Figure 1a shows the characterization of gold nanoparticles using UV-Visible spectroscopy. The UV-Visible spectra of the synthesized gold nanoparticles display a peak at 520nm which is specific for spherical gold nanoparticles owing to the localized surface plasmon resonance (LSPR) occurring in the conduction band when the light of specific wavelength strikes at the surface of these particles.

5.1.2. Electrochemical Characterization of Gold Nanoparticles

For the confirmation of the activity of the gold nanoparticles, nf/ITO was spin-coated with a uniform layer of gold nanoparticles (AuNPs), and an electrochemical response was recorded. The anodic peak current of nf/ITO (0.165mA), increases to 0.212mA for AuNPs/nf/ITO surface, indicating the presence of highly conductive gold nanoparticles on the electrode. (Figure 1b)

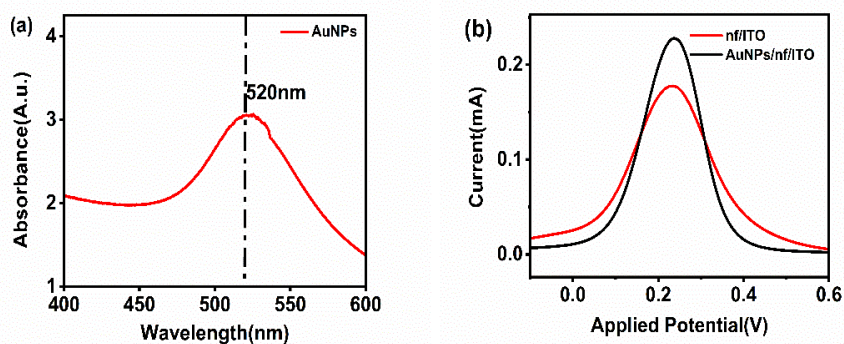


Figure 1. a) UV-Visible spectroscopy of gold nanoparticles. b) Electrochemical characterization of nf/ITO and AuNPs/nf/ITO.

5.2. Electrochemical Characterization of the Fabricated Immunosensor

For each deposited layer, the electrode was electrochemically characterized using differential pulse voltammetry carried out at a voltage range of -0.3V to 0.6V with a step potential of 0.005V and a scan rate of 0.1V/s in 5mM Ferro/Ferricyanide solution $[\text{Fe}(\text{CN})_6]^{3-/4-}$ prepared in PBS. Due to the conductive nature of bare ITO, it gives a peak current of 0.18mA . On the deposition of the biopolymeric layer on the electrode, the current decreases to 0.16mA . To improve the overall conductivity and the charge transfer; a layer of synthesized gold nanoparticles (AuNPs) was spin-coated onto the electrode to form AuNPs/nf/ITO which gives an electrochemical response of 0.21mA . AuNPs/nf/ITO was then considered as a base for the immobilization of optimized concentration (600ngmL^{-1}) of the capture probe, (Spro), for 60min to form Spro/AuNPs/nf/ITO. Following the

immobilization of Spro, the electrode was incubated with BSA (Bovine Serum Albumin,) for 45 min to block the non-specific binding sites and form BSA/Spro/AuNPs/nf/ITO which decreases the electrochemical response to 0.154 mA. The probe BSA/Spro/AuNPs/nf/ITO was used to detect the analyte, CoV2-Ab. To enhance the detection range and sensitivity of the electrode, HRP-pAb was used as a signal probe in the immunosensor HRP-pAb/CoV2-Ab/BSA/Spro/AuNPs/nf/ITO which can be observed with an increase in its electrochemical response. (Figure 2).

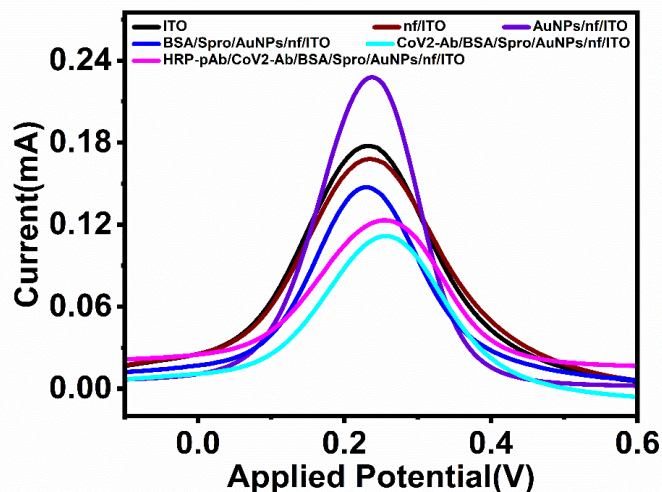


Figure 2. Electrochemical characterization of the fabricated, HRP-pAb/CoV2-Ab/BSA/Spro/AuNPs/nf/ITO immunosensor.

5.3. Analytical Performance of the Immunosensor

5.3.1. Optimization of H₂O₂

H₂O₂ was used as a substrate for the activation of HRP in HRP-pAb/CoV2-Ab/BSA/Spro/AuNPs/nf/ITO. To optimize the concentration and volume of H₂O₂, the immunosensor was electrochemically analyzed by spiking varied concentrations (5%–20%) and volume (100 μl–300 μl) of H₂O₂, to get a maximum response at 200 μl of 5% H₂O₂ concentration as seen in Figure 3(a,b).

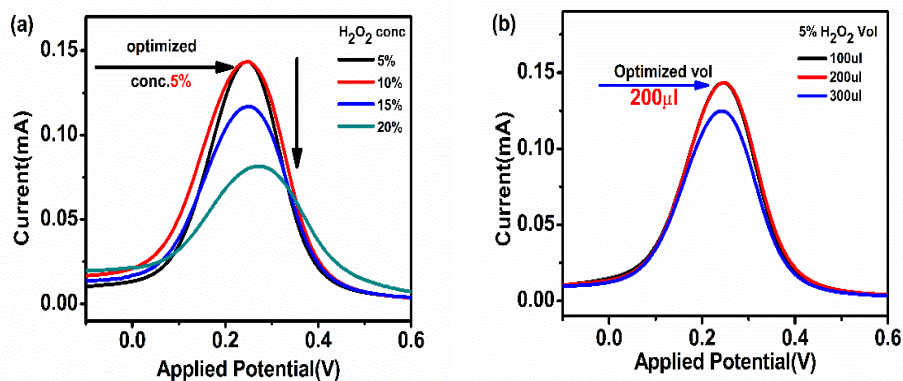


Figure 3. a) Concentration b) volume optimization of the substrate H₂O₂ used to activate HRP in HRP-pAb/CoV2-Ab/BSA/Spro/AuNPs/nf/ITO.

5.3.2. Response Study

The sensor applicability was tested for the detection of different concentrations of CoV2-Ab. The electrochemical response for BSA/Spro/AuNPs/nf/ITO was recorded, and

a decrease in current was recorded on increasing concentration of CoV2-Ab within a linear range of 25–80 ngmL⁻¹ above it no further change was observed in the electrochemical response as seen in Figure 4(a,b). Further, to enhance the range of detection and sensitivity, CoV2-Ab/BSA/Spro/AuNPs/nf/ITO was incubated with the electro-active probe-antibody conjugate (HRP-pAb). Initially, a blank reading was recorded for the probe BSA/Spro/AuNPs/nf/ITO with HRP-pAb, giving an electrochemical response of 0.17 mA. Following this, a varied concentration of CoV2-Ab was tested on HRP-pAb/CoV2-Ab/BSA/Spro/AuNPs/nf/ITO which displays an increase in anodic peak current within a linear range of 10–100ngmL⁻¹, above it no significant changes observed on a further increase of CoV2-Ab concentrations. A calibration curve was prepared for anodic peak response as a function of concentration. The anodic peak current for the blank is higher for immunosensor HRP-pAb/CoV2-Ab/BSA/Spro/AuNPs/nf/ITO, as for blank analysis polyclonal antibody HRP-pAb interacts directly with the capture probe Spro. HRP-pAb binds with a larger number to Spro, generating a high electrochemical response. However, during the analysis, the presence of analyte (CoV2-Ab), which is a biomolecule, creates a hindrance in the transfer of charge. Hence, decrease in conductivity of the immunosensor in comparison to blank was observed. The immunosensor displays a detection range of 10–100 ngmL⁻¹, with linearity R² of 0.96, high sensitivity of 0.013 × 10⁻³ mA ng⁻¹ mLmm⁻² and low limit of detection (LOD) of 3.59 ngmL⁻¹ and quantification (LOQ) 11.84 ngmL⁻¹. (Figure 5(a,b)).

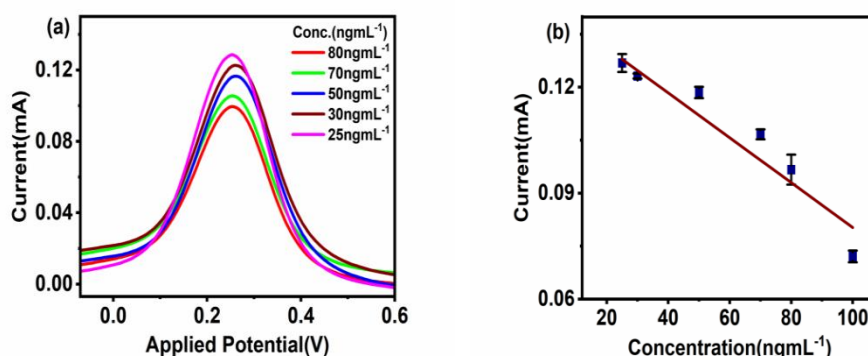


Figure 4. Response study a) Differential Pulse Voltammery b) Calibration curve for the fabricated, BSA/Spro/AuNPs/nf/ITO against CoV2-Ab.

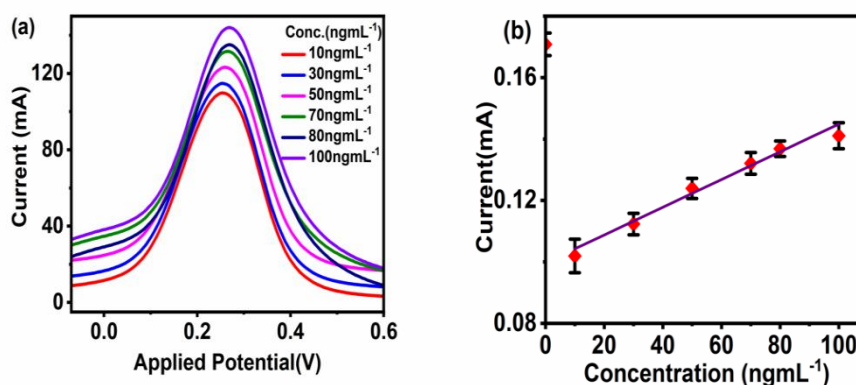


Figure 5. Response study a) Differential Pulse Voltammery b) Calibration curve for the fabricated, HRP-pAb/CoV2-Ab/BSA/Spro/AuNPs/nf/ITO immunosensor against CoV2-Ab.

5.4. Stability Study

The electrochemical response of fabricated immunosensor electrodes was recorded for 30 days at a regular interval of 4 days. The results indicated the electrodes are highly

stable for 30 days as only a 2–4% deviation of results was observed till the 20th day, which consecutively increased up to 10% till the 30th day owing to the denaturation of the protein structure. (Figure 6)

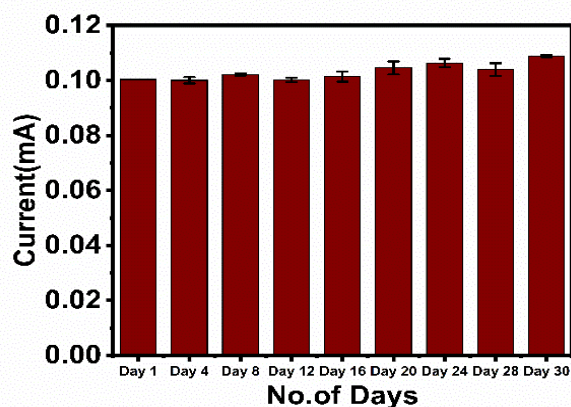


Figure 6. Stability study for the fabricated immunosensor, HRP-pAb/CoV2-Ab/BSA/Spro/AuNPs/nf/ITO.

6. Conclusion:

A nanostructure-decorated electrochemical immunosensor for the rapid quantification of the SARS-CoV2 antibody has been fabricated. The strategy employed for the detection of the viral antibody is the specific interaction of SARS-CoV2 spike receptor binding protein to its antibody. For the fabrication of the immunosensor, the surface properties of the electrode have been enhanced using gold nanoparticles. Further, in the presence of the conjugated secondary antibody; the detection of the antibody concentration ranges from 10–100 ngmL⁻¹ with high linearity ($R^2=0.96$) and sensitivity of $0.013 \times 10^{-3} \text{ mA ng}^{-1} \text{ mLmm}^{-2}$ with a limit of detection (LOD=3.59 ngmL⁻¹ and Quantification (LOQ=11.84 ngmL⁻¹) and stability (30 days). The fabricated immunosensor has a high potential for miniaturization and can be configured with a mobile phone-based interface for on-the-spot, rapid, and quantitative detection.

Funding: The project was funded by BRNS

Conflict of interest: There is no conflict of interest among the Authors

Acknowledgments: We would like to thank BRNS for funding and Amity University Uttar Pradesh for the lab support.

References

1. He, F.; Deng, Y.; Li, W. Coronavirus disease 2019: What we know?. *J. Med Virol.* **2020**, *92*, 719–725. <https://doi.org/10.1002/jmv.25766>.
2. Zhu, H.; Zhang, L.; Ma, Y.; Zhai, M.; Xia, L.; Liu, J.; Yu, J.; Duan, W. The role of SARS-CoV-2 target ACE2 in cardiovascular diseases. *J. Cell. Mol. Med.* **2021**, *25*, 1342–1349. <https://doi.org/10.1111/jcmm.16239>.
3. Ni, W.; Yang, X.; Yang, D.; Bao, J.; Li, R.; Xiao, Y.; Hou, C.; Wang, H. Liu, J.; Yang, D.; et. al. Role of angiotensin-converting enzyme 2 (ACE2) in COVID-19. *Critical Care* **2020**, *24*, 1–10. <https://doi.org/10.1186/s13054-020-03120-0>.
4. Leech, D. Affinity Biosensors. **1994**. Available online: <https://pubs.rsc.org/en/content/articlelanding/1994/cs/cs9942300205/unauth> (accessed on 21 May 2023)
5. Charles J.; Janeway, A.; Travers, P.; Walport, M.; Shlomchik, M.J. The interaction of the antibody molecule with specific antigen. **2001**. Available online: <https://www.ncbi.nlm.nih.gov/books/NBK27160/> (accessed on 5 April 2023).
6. Payandehpeyman, J.; Parvini, N.; Moradi, K.; Hashemian, N. Detection of SARS-CoV-2 Using Antibody–Antigen Interactions with Graphene-Based Nanomechanical Resonator Sensors, Cite This: *ACS Appl. Nano Mater.* **2021**, *2021*, 6189–6200. <https://doi.org/10.1021/acsanm.1c00983>.
7. Xu, L.; Li, D.; Ramadan, S.; Li, Y.; Klein, N. Facile biosensors for rapid detection of COVID-19. *Biosens. Bioelectron.* **2020**, *170*, 112673. <https://doi.org/10.1016/j.bios.2020.112673>.

8. Kudr, J.; Michalek, P.; Ilieva, L.; Adam, V.; Zitka, O. COVID-19: A challenge for electrochemical biosensors. *TrAC Trends in Anal. Chem.* **2021**, *136*, 116192. <https://doi.org/10.1016/j.trac.2021.116192>.
9. Samson, R.; Navale, G.R.; Dharne, M.S. Biosensors: frontiers in rapid detection of COVID-19. *3 Biotech* **2020**, *10*, 385. <https://doi.org/10.1007/s13205-020-02369-0>.
10. ZRahmati, Z.; Roushani, M.; Hosseini, H.; Choobin, H. Electrochemical immunosensor with Cu₂O nanocube coating for detection of SARS-CoV-2 spike protein. *Microchimica Acta* **2021**, *188*, 1–9. <https://doi.org/10.1007/s00604-021-04762-9>/Published.
11. Sundeep, D.; Varadharaj, E.K.; Umadevi, K.; Jhansi, R. Role of Nanomaterials in Screenprinted Electrochemical Biosensors for Detection of Covid-19 and for Post-Covid Syndromes. *Ecs Adv.* **2023**, *2*, 016502. <https://doi.org/10.1149/2754-2734/acb832>.
12. Vadlamani, B.S.; Uppal, T.; Verma, S.C.; Misra, M. Functionalized TiO₂ nanotube-based electrochemical biosensor for rapid detection of SARS-CoV-2. *Sensors* **2020**, *20*, 5871. <https://doi.org/10.3390/s20205871>.
13. Nasrollahzadeh, M.; Sajjadi, M.; Soufi, G.J.; Iravani, S.; Varma, R.S. Nanomaterials and nanotechnology-associated innovations against viral infections with a focus on coronaviruses. *Nanomaterials* **2020**, *10*. <https://doi.org/10.3390/nano10061072>.
14. Beduk, T.; Beduk, D.; de Oliveira Filho, J.I.; Zihnioglu, F.; Cicek, C.; Sertoz, R.; Arda, B.; Goksel, T.; Turhan, K.; Salama, K.N.; et al. Rapid Point-of-Care COVID-19 Diagnosis with a Gold-Nanoarchitecture-Assisted Laser-Scribed Graphene Biosensor. *Anal. Chem.* **2021**, *93*, 8585–8594. <https://doi.org/10.1021/acs.analchem.1c01444>.
15. Ramanathan, S.; Gopinath, S.C.; Ismail, Z.H.; Arshad, M.M.; Poopalan, P. Aptasensing nucleocapsid protein on nanodiamond assembled gold interdigitated electrodes for impedimetric SARS-CoV-2 infectious disease assessment. *Biosens. Bioelectron.* **2022**, *197*, 113735.
16. Funari, R.; Chu, K.Y.; Shen, A.Q. Detection of antibodies against SARS-CoV-2 spike protein by gold nanospikes in an opto-microfluidic chip. *Biosens. Bioelectron.* **2020**, *169*, 112578.
17. Bahrani, S.; Razmi, Z.; Ghaedi, M.; Asfaram, A.; Javadian, H. Ultrasound-accelerated synthesis of gold nanoparticles modified choline chloride functionalized graphene oxide as a novel sensitive bioelectrochemical sensor: Optimized meloxicam detection using CCD-RSM design and application for human plasma sample. *Ultrason. Sonochemistry* **2018**, *42*, 776–786. <https://doi.org/10.1016/j.ultsonch.2017.12.042>.
18. Ghaffarlou, M.; İlk, S.; Hammamchi, H.; Kıraç, F.; Okan, M.; Güven, O.; Barsbay, M. Green and Facile Synthesis of Pul-lulan-Stabilized Silver and Gold Nanoparticles for the Inhibition of Quorum Sensing. *ACS Appl Bio Mater.* **2022**, *5*, 517–527. https://doi.org/10.1021/ACSABM.1C00964/SUPPL_FILE/MT1C00964_SI_001.PDF.
19. Cheng, H.W.; Skeete, Z.R.; Crew, E.R.; Shan, S.; Luo, J.; Zhong, C.J. Synthesis of Gold Nanoparticles. *Compr. Anal. Chem.* **2014**, *66*, 37–79. <https://doi.org/10.1016/B978-0-444-63285-2.00002-X>.
20. Dong, J.; Carpinone, P.L.; Pyrgiotakis, G.; Demokritou, P.; Moudgil, B.M. Synthesis of precision gold nanoparticles using Turkevich method. *KONA Powder Part. J.* **2020**, *37*, 224–232. <https://doi.org/10.14356/kona.2020011>.
21. Shi, L.; Buhler, E.; Boué, F.; Carn, F. How does the size of gold nanoparticles depend on citrate to gold ratio in Turkevich synthesis? Final answer to a debated question *J. Colloid Interface Sci.* **2017**, *492*, 191–198. <https://doi.org/10.1016/J.JCIS.2016.10.065>

Disclaimer/Publisher's Note: The statements, opinions and data contained in all publications are solely those of the individual author(s) and contributor(s) and not of MDPI and/or the editor(s). MDPI and/or the editor(s) disclaim responsibility for any injury to people or property resulting from any ideas, methods, instructions or products referred to in the content.
